Colloid Polym Sci (2005) 283: 1371–1375
DOI 10.1007/s00396-005-1330-5

SHORT COMMUNICATION

Junchun Li
Jianling Zhang
Haixiang Gao
Buxing Han
Liang Gao

Nonaqueous microemulsion-containing ionic liquid [bmim][PF_6] as polar microenvironment

Received: 08 November 2004
Accepted: 04 March 2005
Published online: 28 June 2005

J. Li · J. Zhang · H. Gao · B. Han (✉)
L. Gao
The Center for Molecular Science,
Institute of Chemistry,
The Chinese Academy of Sciences,
Beijing 100080, People's Republic of China
E-mail: Hanbx@iccas.ac.cn
Tel.: +86-10-62562821
Fax: +86-10-62559373

Abstract The phase behavior of toluene/Triton X-100 (TX-100)/1-butyl-3-methylimidazolium hexafluorophosphate([bmim][PF6]) was studied. It was demonstrated that the single-phase microemulsion area covered about 75% of the phase diagram at 25 °C. Electrical conductivities of the system with different *w* ([bmim][PF6]-to-TX-100 molar ratio) values were determined, and the results were used to locate the sub-regions of the single-phase microemulsion. The results showed that a transform from [bmim][PF6]-in-oil ([bmim][PF6]/O) microstructure via a bicontinuous region to an oil-in-[bmim][PF6] (O/[bmim][PF6]) microstructure occurred with the increase of Φ (weight fraction of TX-100 and [bmim][PF6] in the system). The aggregate size of the reverse microemulsions of [bmim][PF6]/O was determined using small-angle X-ray scattering. The results showed that the size of the reverse microemulsions depended markedly on the *w* values.

Keywords Nonaqueous microemulsion · Ionic liquid · Microstructure

Introduction

Microemulsions are thermodynamic stable mixtures of two immiscible solvents (nonpolar and polar) stabilized by amphiphilic molecules or surfactants. They have wide applications in separation science, reaction engineering [1], environmental science [2], and material sciences [3, 4] with some unique advantages.

In the majority of the studies of traditional microemulsions, water was used as the polar component. In recent years, attempts have been made to prepare and study waterless microemulsions. In this effort, water has been replaced by polar organic solvents [5–9]. These nonaqueous microemulsions are essentially oil continuous and have attracted much recent interest from both theoretical (thermodynamics, particle interactions) and practical (potential use as novel reaction media) viewpoints [8]. Nonaqueous microemulsion systems have some advantages over the aqueous ones. They are especially useful when water should be avoided.

The room temperature ionic liquids (ILs) offer great potential as environmentally acceptable media for the process industry [10]. They have been extensively investigated for electrochemical applications and as reaction media for catalytic processes [11–18]. However, many ILs show miscibility gaps with nonpolar solvents. Combination of ILs, surfactants, and nonpolar solvents to form micelles or microemulsion systems is a promising research area. Several papers related to both ILs and emulsions have been published. Davis and coworkers

have discovered that some fluorous ILs could act as surfactants and promoted the stabilization of perfluorocarbons in a conventional ionic liquid, 1-hexyl-3-methylimidazolium hexafluorophosphate [19]. Binks et al. have reported novel emulsions of ILs stabilized solely by silica nanoparticles [20]. Recent study has revealed that some surfactants may form aggregations or micelles in ILs [21, 22].

We are very interested in the reverse micelles with an IL as polar cores or the reverse microemulsions with nano-sized IL droplets dispersed in oil continuous phase because they may have some unknown properties and find various potential applications due to the unique features of ILs and microemulsions. In previous communication [23], we studied phase behavior of cyclohexane/1-butyl-3-methylimidazolium tetrafluoroborate ([bmim][BF_4])/Triton X-100 (TX-100) system, and the reverse microemulsions with [bmim][BF_4] polar cores were characterized by dynamic light-scattering, freeze-fracturing electron microscopy. Can other ILs also form polar cores in other suitable organic solvents? In this work, we studied the phase behavior and electrical conductivity of toluene/TX-100/[bmim][PF_6] system, and small-angle X-ray scattering (SAXS) technique has been used to characterize the structure and size of the reverse microemulsions of TX-100 in toluene with [bmim][PF_6] cores.

Experimental section

Materials

[bmim][PF6] was synthesized according to the method reported in the literature [24], and the density and molecular weight are 1.37 g/ml and 284.2 g/mol, respectively. TX-100 ($CH_3C(CH_3)_2CH_2C(CH_3)_2C_6H_4(OCH_2CH_2)_{9.5}OH$, $M = 646.86$ g/mol, $d^{20} = 1.063$ g/ml), which is a typical nonionic surfactant, was obtained from Beijing Chemical Reagent Corporation. Toluene ($M = 92.14$ g/mol, $d^{20} = 0.867$ g/ml) was obtained from Beijing Chemical Reagent Corporation. Before being used, [bmim][PF6] and TX-100 were dehydrated under vacuum at 70 °C until their weights were independent of drying time. In all the experiments the samples were sealed in order to avoid absorption of moisture.

Procedures to determine phase diagram

Ternary phase diagram of the ternary system was determined at 25.0 ± 0.1 °C by direct observation of the phase behaviour. In a typical experiment, [bmim][PF6] and toluene were added into the glass test tube, and their masses were determined by a balance (OHAUS Co.) with a resolution of 0.0001 g. The test tube was then placed in a constant temperature water bath. After thermal equilibrium had been reached, the solution was shaken. The sample was then titrated with TX-100 until the hazy and milky liquid solution became transparent and completely clear, which was an indication of the formation of the single-phase, and the corresponding composition of the solution was located on the phase boundary. The mass of TX-100 added was also known from the mass difference of the glass test tube before and after adding TX-100. The composition of the solution was easily calculated from the masses of [bmim][PF6], toluene, and TX-100. It was estimated that the accuracy of measurements for the phase boundary composition was better than ±2%.

Electrical conductivity experiment

The apparatus and procedures to determine the electrical conductivities of the nonaqueous microemulsions were similar to those used in our previous work [23]. The cell constant of the electrode used was 0.965 cm^{-1}. A dilution series of these nonaqueous microemulsions was prepared by varying the weight fraction Φ in the range 0.25∼1.0 at a fixed w value ([bmim][PF_6]-to-TX-100 molar ratio). Here, Φ is defined as the weight fraction of TX-100 and [bmim][PF_6] in the system:

$$\Phi = (W_{\mathrm{TX-100}} + W_{[\mathrm{bmim}][\mathrm{PF6}]})/(W_{\mathrm{TX-100}} + W_{[\mathrm{bmim}][\mathrm{PF6}]} + W_{\mathrm{toluene}})$$

SAXS experiment

SAXS experiments were carried out at Beamline 4B9A at the Beijing Synchrotron Radiation Facility (BSRF). The small-angle X-ray scattering station is located 31 m from the source. The station was equipped with a SAXS camera, a detector, an on-line data-acquisition, a controlling system, and an alignment carriage. The data accumulation time was 3 min. The wavelength used was 1.54 Å, and the sample-to-detector distance was 1.495 m. The detailed description of the spectrometer was given elsewhere [25]. In a typical experiment, the desired amount of the reverse microemulsion of toluene/TX-100/[bmim][PF6] was added into the sample cell of Kapton membrane, and the X-ray scattering was recorded at 25.0 °C.

Data analysis of SAXS

The Guinier approximation was often used to obtain the size of the reverse micelles or microemulsions [26–28]. This approximation is based on the fact that the scat-

tering curve shows Gaussian shape at small angles, of which the slope depends on the radius of gyration. After correction of the scattering data by subtraction of the background noise, the following analyses were done. In the lower q region, contributions to the total excess X-ray scattering, $I(q)$, due to microemulsions can arise from two sources: the droplet contribution, which depends solely upon the radius of the droplet, and an appropriate structure factor, which accounts for attractive or repulsive interactions between the droplets. When the system is sufficiently dilute, inter-droplet interactions are negligible. The magnitude of the scattering vector q is given in terms of the scattering angle 2θ by $q = 4\phi \sin \theta/\lambda$, where λ is incident X-ray wavelength, 1.54 Å. For dilute solutions the apparent gyration radius R_g of the micellar core can be obtained by using the Guinier approximation law, which is valid at low q region and can be expressed by Eq. 1 [26, 28–30].

$$\ln[I(q)] = \ln[I(0)] - \frac{(qR_g)^2}{3} \quad (1)$$

where $I(0)$ denotes the scattering intensity extrapolated to zero angle. The Guinier plots give a precise value of the apparent gyration radius only if the representation is linear at small values of q. In this work, by using Guinier plot ($\ln I(q)$ versus q^2) on the data sets in a defined small q range (0.017∼0.032 Å^{-1}) [26, 28], linear regression analysis of the intensity curves was used to obtain R_g values.

Results and discussion

Phase diagram studies

The phase diagram of toluene/TX-100/[bmim][PF6] ternary system at 25.0 °C is illustrated in Fig.1. Above the phase separation boundary line (A, B and C regions), the system exists as a single phase, and the shadow area (D region) is a biphasic region. The total single-phase microemulsion area covers about 75% of the phase diagram. In Fig. 1, the SAXS samples are also indicated using the symbols of (filled circle), (filled star), (filled triangle), (filled square) and (open square)

Electrical conductivity studies

The structures of microemulsions have been an interesting topic for years. The single-phase region of microemulsions can be divided into different sub-regions, such as water (or polar solvent)-in-oil microemulsion region (water or polar solvent droplets dispersed in oil), oil-in-water (or polar solvent) microemulsion region (oil droplets dispersed in water or polar solvent), and

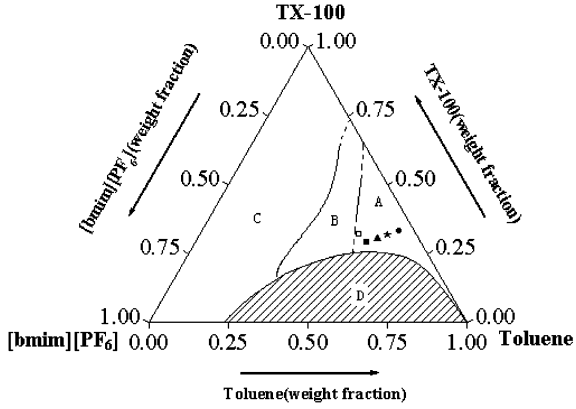

Fig. 1 Phase diagram of toluene/TX-100/[bmim][PF_6] (in weight fraction) at 25.0 °C. **a** [bmim][PF_6]/O microemulsion; **b** bicontinuous region; **c** O/[bmim][PF_6] microemulsion; **d** biphasic region. Symbols (*filled circle*), (*filled star*), (*filled triangle*), (*filled square*) and (*open square*) mark the conditions at which SAXS experiments were carried out

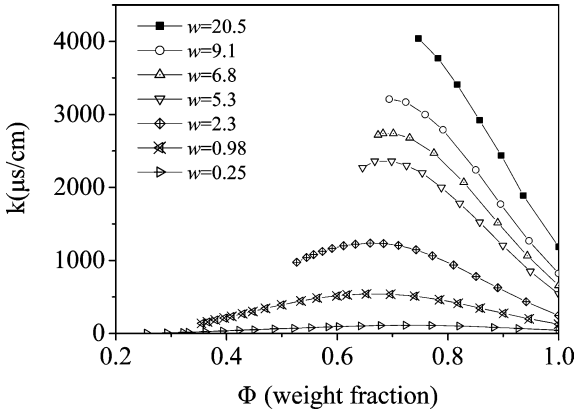

Fig. 2 Variation of conductivity k (μs/cm) vs. Φ (weight fraction of TX-100 + [bmim][PF_6]) for toluene/TX-100/[bmim][PF_6] system with different w values at 25.0 °C

bicontinuous region. The sub-areas can be conveniently located by electrical conductivity measurement [31–33]. In this work, we determined the sub-regions by this method. The variations of conductivity (k) as a function of Φ (weight fraction of TX-100 and [bmim][PF_6]) for the microemulsion with different w values at 25.0 °C are shown in Fig. 2. As expected, k increases with the increase of w values because the conductivity originates mainly from the IL.

The scanning paths with different w values cover the entire single-phase microemulsion, as shown in Fig.3a. The principle to locate the sub-region of the single-phase microemulsion was described by other authors [31–33]. As an example, Fig. 3b shows how to distinguish the sub-regions of the microemulsion on the basis of conductivity data. The figure demonstrates the variation of conductivity k (μs/cm) vs. Φ (weight fraction of TX-100 and

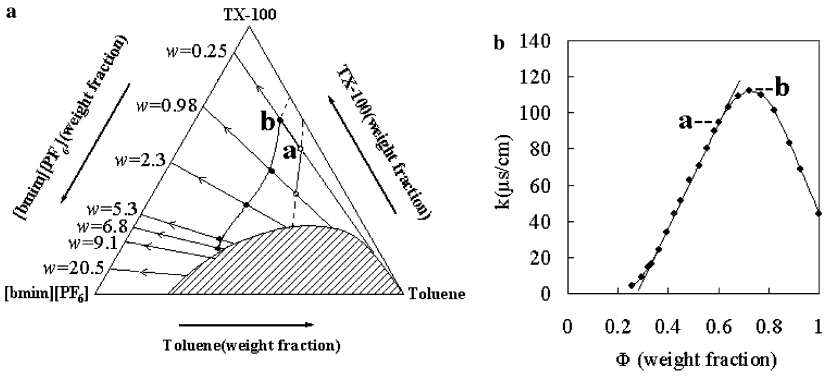

Fig. 3 Scanning paths in conductivity measurements at different w values **a** and variation of conductivity k (μs/cm) vs. Φ (weight fraction of TX-100 + [bmim][PF_6]) at $w = 0.25$ (**b**) for toluene/TX-100/[bmim][PF_6] system at 25.0 °C

[bmim][PF_6]) in the system of toluene/TX-100/[bmim][PF_6] with $w = 0.25$. Up to $\Phi = 0.60$ (Point *a*), the toe at the bottom and the medium linear part are characteristic for a percolative conduction in [bmim][PF_6]/O reverse microemulsion. Past point *a*, k increases more slowly, and reaches a maximum (point *b*) at the content of $\Phi = 0.72$. Then k decreases with increasing Φ as the system enters O/[bmim][PF_6] microemulsion sub-region. Consequently, the conductivity curve between points *a* and *b* indicates the existence of a special conduction mechanism reflecting an intermediary physical state of the system, i.e. bicontinuous region. The composition path corresponding to Fig. 3b is illustrated in Fig. 3a. Microstructure transition points *a* and *b* are also marked in Fig. 3a. The conductivity curve shows that the microemulsion transforms from a [bmim][PF_6]/O microemulsion via a bicontinuous region to an O/[bmim][PF_6] microemulsion. Similarly, we can obtain the microstructure transition points (symbols of open circle and filled circle in Fig. 3a) of the system with different w values on the basis of conductivity data. Using this method, we determined three types of sub-regions in the single-phase microemulsion, [bmim][PF_6]/O microemulsion, bicontinuous region, and O/[bmim][PF_6] microemulsion, corresponding to A, B and C regions in Fig. 1, respectively. It was estimated that the uncertainty to locate the boundaries of region B should be less than ±5%.

SAXS studies

SAXS technique is a useful technique to provide the information on the microstructure of the microemulsion. The SAXS curves of the reverse microemulsions of toluene/TX-100/[bmim][PF_6] ($C_{TX\text{-}100} = 0.31$ mol/l) with different w values and the corresponding Guinier plots of ln $I(q)$ vs. q^2 are shown in Fig. 4. It can be observed that in the small angle region the scattering intensity increases with increasing w values. One of the

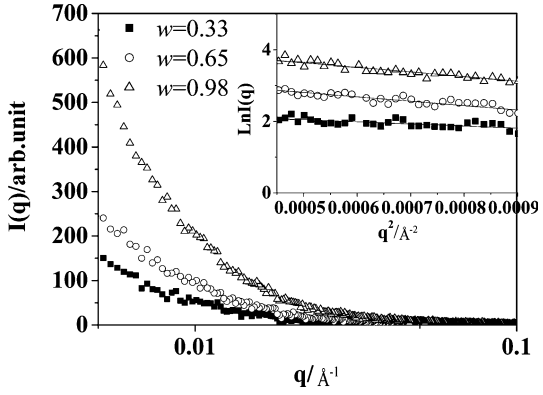

Fig. 4 SAXS curves of reverse microemulsions of toluene/TX-100/[bmim][PF_6] ($C_{TX\text{-}100} = 0.31$ mol/l) system with different w values, the inset shows the corresponding Guinier plots

reasons is due to the increase of micelle size, which will be discussed in the following. The apparent gyration radii (R_g) of the reverse micelles with w values of 0.33, 0.65 and 0.98 are 43.8, 61.4, and 62.3 Å, respectively, which are estimated using Eq. 1. As we can see, the R_g of the reverse micelles increases with increasing w values. It is easy to understand that the micellar core increases with the increasing concentration of [bmim][PF_6] at constant concentration of TX-100. In the defined q range shown in Fig. 4, the linearity of the ln $I(q)$ vs. q^2 is excellent, which in turn proves the validity of using Guinier approximation law in this small-angle region.

We also studied the effect of concentration of surfactant TX-100 on R_g at a fixed w value. Figure 5 shows the SAXS curves and the corresponding Guinier plots of the reverse microemulsions of toluene/TX-100/[bmim][PF_6] with $w = 1.3$ and different concentrations of TX-100. The apparent gyration radii (R_g) of the reverse micelles with TX-100 concentrations of 29 and 33 wt% are 65.7 and 65.9 Å, respectively. Thus, it can be concluded that the concentration of TX-100 has little effect on R_g in certain concentration range.

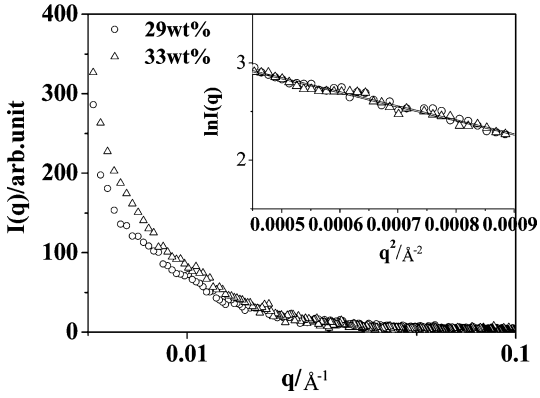

Fig. 5 SAXS curves of the reverse microemulsions of toluene/TX-100/[bmim][PF_6] system with different TX-100 concentrations ($w = 1.3$), the inset shows the corresponding Guinier plots

Conclusion

Phase behavior, conductivity, and SAXS study show that in the toluene/TX-100/[bmim][PF_6] system, reverse micelles with [bmim][PF_6] polar cores can be formed at the suitable conditions. The reverse micelles may have some potential applications in different fields, such as chemical reactions, synthesis of organic and inorganic materials, and extractions and fractionations.

Acknowledgements The authors are grateful to the National Natural Science Foundation of China for their financial support (20133030).

References

1. Candau F, Zekhini Z, Heatley F (1986) Macromolecules 19:1895
2. Monig K, Haegel FH, Schwuger IJ (1996) Tenside Surf Deterg 33:228
3. Wormuth KR, Caldwell LA, Kaler EW (1990) Langmuir 6:1035
4. Kahlweit M (1993) Tenside Surf Deterg 30:83
5. Friberg SE, Podzinsek M (1984) Colloid Polym Sci 262:252
6. Rico I, Lattes A (1984) J Colloid Interface Sci 102:285
7. Fletcher PDI, Galal M, Robinson BH (1984) J Chem Soc Faraday Trans 1 80:3307
8. Schubert KV, Lusvardi KM, Kaler EW (1996) Colloid Polym Sci 274:875
9. Schubert KV, Busse G, Strey R, Kahlweit M (1993) J Phys Chem 97:248
10. Hussey CL (1988) Pure Appl Chem 60:1763
11. Seddon KR (1997) J Chemical Tech Biotech 68:351
12. Chauvin Y, Olivier-Bourbigou H (1995) Chemtech 25:26
13. Abdul-Sada AK, Ambler PW, Hodgson PKG, Seddon KR, Steward NJ (1995) World Pat WO 9521871
14. Chavin Y, Commereuc D, Hirschauer A (1988) French Pat FR 2:611–700
15. Ellis B, Keim W, Wasserscheid P (1999) Chem Commun 337
16. Ambler PW, Hodgson PKG., Stewart NJ (1996) European Pat App EP/0558187A0558181
17. Abdul-Sada AK, Atkins MP, Ellis B, Hodgson PKG, Morgan MLM, Seddon KR (1995) World Pat WO 95/21806
18. Adams CJ, Earle MJ, Seddon KR (1999) Chem Commun 1043
19. Merrigan TL, Bates ED, Dorman SC, Davis JH (2000) Chem Commun 2051
20. Binks BP, Dyab AKF, Fletcher PDI (2003) Chem Commun 2540
21. Anderson JL, Pino V, Hagberg EC, Sheares VV, Armstrong DW (2003) Chem Commun 2444
22. Fletcher KA, Pandey S (2004) Langmuir 20:33
23. Gao HX, Li JC, Han BX, Chen WN, Zhang JL, Zhang R, Yan DD (2004) Phys Chem Chem Phys 6:2914
24. Huddleston JG, Willauer HD, Swatloski RP, Visser AE, Rogers RD (1998) Chem Commun 1765
25. Dong BZ, Sheng WJ, Yang HL, Zhang ZJ (1997) J Appl Cryst 30:877
26. Hirai M, Kawai-Hirai R, Yabuki S, Takizawa T, Hirai T, Kobayashi K, Amemiya Y, Oya M (1995) J Phys Chem 99:6652
27. Hirai M, Kawai-Hirai R, Sanada M, Iwase H, Mitsuya S (1999) J Phys Chem B 103:9658
28. Liu JC, Han BX, Zhang JL, Li GZ, Zhang XG, Wang J, Dong BZ (2002) Eur Chem J 8:1356
29. Eastoe J, Paul A, Nave S, Steytler DC, Robinson BH, Rumsey E, Thorpe M, Heenan RK (2001) J Am Chem Soc 123:988
30. Maitra A (1984) J Phys Chem 88:5122
31. Clausse M, Peyrelasse J, Hell J, Boned C, Lagourette B (1981) Nature 293:636
32. Raj WRP, Sasthav M, Cheung MH (1991) Langmuir 7:2586
33. Kirkpartrick S (1971) Phys Rev Lett 27:1722